Elastic properties prediction of a knitted composite with inlaid yarns subjected to stretching

Gilles Dusserre, Laura Balea, Gérard Bernhart

Elastic properties prediction of a knitted composite with inlaid yarns subjected to stretching: A coupled semi-analytical model

Gilles Dusserre *, Laura Balea, Gérard Bernhart

Université de Toulouse, Mines Albi, ICA (Institut Clément Ader), Campus Jarlard, F-81013 Albi Cedex 09, France

ABSTRACT

Knit reinforced composites cover a large range of mechanical properties thanks to the multitude of structures available. In this paper, a semi-analytical tool is presented allowing to improve the fabric design by assessing the elastic properties of a stretched knit reinforced composite with several inlays. The stretched loop geometry is obtained with a loop stretching model based on the beam theory. A geometric model of the inlays is proposed. These results are used as input data of a mesoscopic scale homogenisation model to assess the composite elastic properties. A comparison of the results to the load–strain curve of a plain knit shows that the modelled loop shape is realistic, and the homogenisation model results agree with experimental data. This tool is used to draw a map of the wale-wise versus course-wise modulus that can help to design a fabric leading to a composite with tailor-made properties.

1. Introduction

Knitting is an efficient process to automatically produce complex shape preforms of technical textile. 3D [1], tubular [2] or holed [3] near net-shape fabrics can be obtained in a single step and provide composites with a large range of properties thanks to the numerous knitting patterns available [4]. Moreover the extensibility of the fabrics allows an easy forming of the knitted preforms [5–7]. The properties of the knit reinforced composites depend on the fibrous architecture and thus on the fibre type, the basis knitted structure [4], the knitting parameters and the insertion of inlaid yarns [8–10], as well as on fabric stretching [11].

For forming simulation purposes, the mechanical properties of knit composites are more likely identified at the macroscopic level as an anisotropic homogenised material [7]. To assess the elastic properties of knit reinforced composites, micro-mechanical models are required in order to take into account the fibrous architecture of the reinforcement at the mesoscopic scale of the loop. Some finite element analysis based approaches have been proposed [12], but most of the works carried out use an analytical method to homogenise a unit cell based on the loop geometry [13]. Rudd et al. [14] combined the model proposed by Krenchel [15] with the rule of mixture to approximate the tangent modulus of plain knit composites using a simple geometric description of the loop using straight lines and arcs of a circle. The yarn is assumed to be an unidirectional rod that contributes to the stiffness of the composite according to an efficiency factor depending on the angle between the local direction of the yarn and the loading direction. Ramakrishna et al. [16,17] improved this approach by describing the 3D loop geometry using the model of Leaf and Glaskin [18]. The unit cell is thus composed of a matrix part and a curved impregnated yarn idealized as a unidirectional lamina. The yarn is then discretized into short straight segments whose contribution to the stiffness of the composite is a function of their angle with the loading direction. This so-called 'cross-over model' has been widely exploited to successfully investigate the behaviour of various knit reinforced composites, see [13] and references within. It is proposed here to enlarge the application range of this model by coupling it to a model of the knitted fabric biaxial stretching in order to take into account an accurate geometric description of the loop in the stretched state.

For knitting [7] or forming [19–21] simulation purposes, some finite element based approached have been carried out allowing to describe the loop shape with various degrees of accuracy. Some analytical approaches have also been developed in the seventies, based on an analysis of the static equilibrium of the loop. The loads acting on the yarn in the loop have been formalized allowing to model the behaviour of weft knit under biaxial [22,23] or uniaxial [24,25] extension loads. More recently, a 2D analytical model was proposed by Hong et al. [26] allowing to simulate the geometry of the loop in a stretched state, either under biaxial or uniaxial

* Corresponding author. Address: Ecole des Mines d'Albi, Institut Clément Ader, Campus Jarlard – Route de Teillet, 81013 Albi Cedex 9, France. Tel.: +33 563 493 309; fax: +33 563 493 242.

E-mail address: gilles.dusserre@mines-albi.fr (G. Dusserre).

loading. This model will be used in the present paper to describe the geometry of the loop.

This work aims to propose a rather simple tool able to assess the elastic properties of plain knit reinforced composites in order to help the designer to chose the most relevant knitted reinforcement to build a composite with tailor-made elastic properties for a given application. Plain knit is chosen as the basis structure since it is able to provide a large range of properties, from almost isotropic to orthotropic with greater stiffness either in wale or course-wise directions using inlaid yarns [10,27]. The rather simple but efficient model proposed in this paper takes into account the yarn diameter and the fibre elastic properties, the plain knit basis structure, the inlaid yarns with float and tuck stitches and the biaxial stretching of the knit resulting from the forming step. For that purpose, the geometry of the unit cell is provided by a model of the biaxial stretched plain knit, enriched by a geometric description of the inlaid yarns. It feeds an homogenisation model to assess the elastic properties of the composite.

2. Modelling the load-extension behaviour of a plain-knit

The knit is assumed to be composed of loops of yarn, idealized as an homogeneous elastic rod of circular cross-section. The bending of the yarn is assumed to be the only deformation mechanism that occurs in the loop, as it is the main mechanism that controls the first step of the behaviour, i.e. a large strain under a low load. The yarn is thus characterized by its diameter, d, and its bending stiffness, denoted $B = EI$, where E is the Young's modulus of the fibre and I is the second moment of area of the yarn with respect to an axis perpendicular to the yarn axis. The value of d does not affect significantly the behaviour of the knit before jamming, but mainly controls the deformation at which the jamming occurs in the wale direction [28]. The present work mainly focuses on the deformation before jamming. For the sake of simplicity, the diameter d is thus approximated using the yarn technical data assuming a perfect hexagonal packing of the filaments, according to Eq. (1), where d_f and N_f are respectively the average diameter and the number of filaments into the yarn.

$$d = d_f \sqrt{\frac{2\sqrt{3}}{\pi} N_f} \qquad (1)$$

With the same goal in mind, it is proposed here to simply assess the second moment of area of the yarn from the filament diameter and number. It is assumed that the energy required to bend the yarn is the sum of the energies required to bend each filament with the same curvature as the yarn neutral axis, i.e. no tension or compression arises in the filament as a result of the yarn bending. The second moment of area of the yarn, I, is thus the sum of the second moments of area of each filament, Eq. (2). This strong assumption will be discussed regarding the results of the model compared to experimental data.

$$I = N_f \frac{\pi d_f^4}{64} \qquad (2)$$

The plain-knit is characterized by the average width of a wale, W, the average height of a course, C, and the average yarn length per loop, L. W is the width of the fabric divided by the number of wales, C is the length of the fabric divided by the number of courses, and L is the length of yarn in the fabric (assessed by the ratio between the fabric mass and the yarn linear density) divided by the number of loops.

2.1. Geometric parameterization and static equilibrium of a loop [26]

For the sake of simplicity, the plain-knit will be schematized by a plane geometry, since the analysis only focuses on the effect of stretching the knit in-plane. Considering the symmetries of the plain-knit structure, the representative volume element is comprised of two quarters of loop, symmetric with respect to the contact point of the two adjacent loops. The static equilibrium analysis will be performed on one quarter of the loop. Fig. 1 shows a schematic of the geometric parameterization and the external loads acting on this system under equilibrium, and defines the X-axis parallel to the course direction, and the Y-axis parallel to the wale direction. The system is subjected at point C to a load T parallel to the X-axis and to a torque M, allowing to keep the symmetry about the Y-axis, (the tangent to the neutral axis at point C is parallel to the X-axis). The contact force between the two quarter loop segments, R, is assumed to apply at point B of the neutral axis of the yarn, since the yarn diameter is small compared to the loop size. The friction is neglected and R is thus assumed to be perpendicular to the tangent of the neutral axis at point B. The contact is assumed to be punctual and no torque is thus transmitted between the two loops at B, at least for this in-plane analysis. Finally, a load P applies at point A, the inflection point of the yarns neutral axis. The assumption of an arbitrary load direction is taken in the plane. As the yarn is not curved at this point, no torque is acting.

Three angles are introduced to parameterize the geometry of the quarter of loop. β is the angle between the tangent to the yarn at point B and the X-axis, γ is the angle between the direction of the force P and the negative direction of the X-axis, and α is the angle between the tangent to the yarn at point A and the X-axis.

Geometry based considerations allow to write a first set of four equations relating the known parameters W, C, L and d to the angle β, the coordinates of points A and B, and the length of the segments AB and BC. The static equilibrium of the quarter of loop allows to express T, R and M as functions of the load P, the angles β and γ, and the distances y'_{AB} and y_{BC}. The differential equation $B\partial\theta/\partial s = M_z$ relating the bending moment M_z to the curvature $\partial\theta/\partial s$ (s is the curvilinear abscissa and θ is the section rotation) and the bending rigidity B of the yarn can be integrated separately on each segment AB and BC allowing to obtain on the one hand, the coordinates of the points A and B, and the length of the segment AB, and on the other hand, the length of the segment BC. All the required calculus is detailed in Ref. [26] from which the notations, assumptions and developments used in the present paper have been borrowed. The final set of equations obtained is given in Eqs. (3)–(5), where functions C_1, C_2, C_3 and C_4 are defined in Eqs. (6)–(9). $F(\varepsilon_i, \varphi_i)$ and
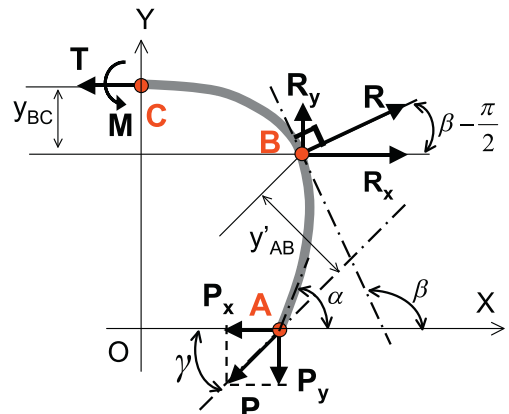
Fig. 1. Geometric parameterization of the external loads acting on a quarter loop. (For interpretation of the references to colour in this figure legend, the reader is referred to the web version of this article.)

$E(\varepsilon_i, \varphi_i)$ are respectively the incomplete elliptic integral of the first and second kind defined by Eqs. (10), (11), $e(\varepsilon_1, \phi_{1B}) = E(\varepsilon_1, \pi/2) - E(\varepsilon_1, \phi_{1B})$, $f(\varepsilon_1, \phi_{1B}) = F(\varepsilon_1, \pi/2) - F(\varepsilon_1, \phi_{1B})$, $k_1 = \cos\gamma + \sin\gamma \tan\beta$, $k_2 = k_1 + k_1 \cos\beta + 2\varepsilon_1^2 \cos^2 \phi_{1B}$, $\varepsilon_1 = \cos[(\alpha - \gamma)/2]$, $\varepsilon_2 = \sqrt{2k_1/k_2}$, $\phi_{1B} = \arcsin\{\cos[(\beta - \gamma)/2]/\varepsilon_1\}$ and $\phi_{2B} = (\pi - \beta)/2$. All these equations provide a complete description of the loop geometry and allow the calculation of the loads acting on the loop, $P = 16BC_4^2/L^2$ and $T = -k_1 P$.

$$\frac{L}{W} = \frac{C_4}{C_1 - C_3} \tag{3}$$

$$\frac{L}{C} = \frac{2C_4}{C_2 + C_3 \cot\beta} \tag{4}$$

$$\frac{L}{d} = 2\frac{C_4}{C_3} \sin\beta \tag{5}$$

$$C_1 = \sqrt{\frac{2}{k_2}} \left[\frac{2}{\varepsilon_2^2} E(\varepsilon_2, \phi_{2B}) + \left(1 - \frac{2}{\varepsilon_2^2}\right) F(\varepsilon_2, \phi_{2B}) \right] \tag{6}$$

$$C_2 = [f(\varepsilon_1, \phi_{1B}) - 2e(\varepsilon_1, \phi_{1B})] \sin\gamma + 2\varepsilon_1 \cos\phi_{1B} \cos\gamma \tag{7}$$

$$C_3 = [f(\varepsilon_1, \phi_{1B}) - 2e(\varepsilon_1, \phi_{1B})] \cos\gamma + 2\varepsilon_1 \cos\phi_{1B} \sin\gamma \tag{8}$$

$$C_4 = f(\varepsilon_1, \phi_{1B}) + \sqrt{\frac{2}{k_2}} F(\varepsilon_2, \phi_{2B}) \tag{9}$$

$$E(\varepsilon_i, \phi_i) = \int_0^{\phi_i} \sqrt{1 - \varepsilon_i^2 \sin^2\phi} \, d\phi \tag{10}$$

$$F(\varepsilon_i, \phi_i) = \int_0^{\phi_i} \frac{d\phi}{\sqrt{1 - \varepsilon_i^2 \sin^2\phi}} \tag{11}$$

2.2. Plain-knit stretching modelling

The quasi-static stretching of a plain-knitted fabric is assumed to be a sequence of equilibrium states. The equations above can thus apply to any stretched state of the fabric throughout a biaxial or uniaxial test. The Young's modulus of the filaments, E, is known and the geometric characteristics of the yarn, d and I, are assessed through Eqs. (1), (2). If the angles α, β and γ are known, it is possible to calculate L (Eqs. 5, 8, 9) and then W (Eqs. 3, 6, 8, 9) and C (Eqs. (4), (7)–(9)). The direct problem is solved by discretizing the yarn into 500 segments of equal length in order to compute the elliptic integrals using the trapezoidal rule. The simulation of a stretching experiment thanks to this set of equations requires the inverse problem to be solved, i.e. to find the values of α, β and γ that lead to the values of three known parameters, allowing the forces acting on the loop to be computed. The three known parameters must be carefully chosen depending on the experiment under consideration. Nevertheless, the first step is an updating of the initial values of α, β and γ corresponding to the unloaded state, irrespective of the experiment.

2.2.1. Initialization and solving procedure

In the unloaded state, the initial values of C and W, denoted C_0 and W_0, can be measured directly on the fabric and L can be deduced from the fabric mass. A Newton–Raphson method is used to solve the inverse problem and find the initial values of α, β and γ, denoted α_0, β_0 and γ_0, that correspond to the experimental values C_0, W_0 and L, Fig. 2a. The forces acting on the loop when the fabric is not loaded are then available.

2.2.2. Biaxial stretching

In the case of a uniform biaxial stretching, the calculation strategy is the same as the initialization procedure. C and W are imposed during the experiment and L is assumed to be the same as in the unloaded state. The inverse method allows thus to compute the values of α, β and γ for any biaxial stretched state, Fig. 2b. The loads acting on the loop when the fabric is biaxially stretched are then available.

2.2.3. Uniaxial elongation in the course-wise direction

In the case of a uniaxial stretching in the course-wise direction, L is still assumed to be constant, and W is imposed by the course-wise strain. Nevertheless C varies in an undefined manner and the problem is thus undetermined. Solving the problem requires to impose a third parameter. Hong et al. [26] proposed to impose a constant length of the segment BC, assuming that no sliding occurs at the contact point between the two quarter loops. The inverse method allows thus to compute the values of α, β and γ for any course-wise stretched state, Fig. 2c. The forces acting on the loop when the fabric is stretched in the course-wise direction are then available.

2.2.4. Uniaxial elongation in the wale-wise direction

The last case under study is the wale-wise elongation. As for the previous case, L is still assumed to be constant, and C is now imposed by the wale-wise strain, whereas W varies in an undefined manner. The deformation mechanism involves a sliding of the contact point up to the jamming of the loop. Before the jamming, the third parameter imposed is the force T, assumed by Hong et al. [26] to be constant during this step. The jamming occurs when two interlacing quarter loops are in contact, i.e. when the width of a wale reaches the value $4d$ if the yarn is supposed to have a circular cross-section. For an incompressible yarn, once jamming has occurred, the width of a wale, W, is constant and set to the value $4d$. The inverse method allows the computation of the values of α, β and γ for any wale-wise stretched state, Fig. 2d. The forces acting on the loop when the fabric is stretched in the wale-wise direction are then available.

2.3. Comparison between experimental and theoretical results

2.3.1. Experimental data

The fabrics tested in course and wale-wise extension to validate the results of the model are 5 gauge plain-knits made of 600 tex yarns of Basaltex® BCF basalt fibres. The yarns are comprised of 1672 fibres of diameter 13 μm. According to the manufacturers datasheet, the density of the basalt is 2700 kg m^{-3} and its Young's modulus is 84 GPa. According to Eq. (1), the theoretical yarn diameter, d, is 0.56 mm. According to Eq. (2), the theoretical bending stiffness, B, is 0.197 N mm^2. The surface density of the plain-knit is 690 g m^{-2}, its thickness is 1.45 mm, the average width of a wale, W, is 4.40 mm, the average height of a course, C, is 2.65 mm, and the average yarn length per loop, L, is 13.1 mm. The knit was tested in course and wale-wise directions according to the experimental procedure described in [10]. The experimental data are compared to the results of the model using the aforementioned data in the next subsection.

2.3.2. Theoretical results and comparison to tensile tests

Figs. 3 and 4 compare the load/strain curves computed with the model and the experimental ones. In the wale-wise direction, Fig. 3, both behaviour ranges (before and after jamming) are described, and the strain at which jamming point occurs are similar, around 60%. Nevertheless the modelled behaviour is too linear in both domains, and the sudden slope change at jamming is not physical since this phenomena is actually combined with a
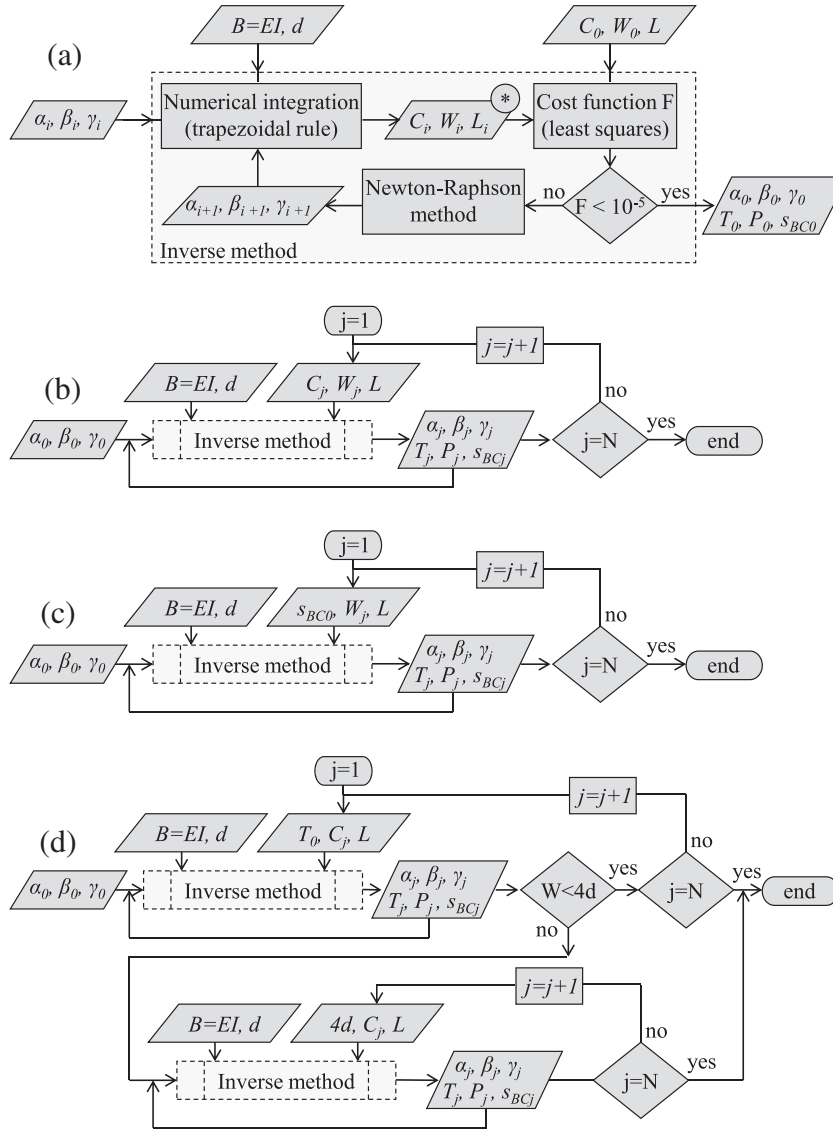
Fig. 2. Algorithms for the simulation of the initial state (a), a biaxial elongation (b), an uniaxial elongation in the course-wise direction (c) and in the wale-wise direction (d). N is the number of increment and the sub-process "Inverse method" is detailed only for the initial state. *: Computed values of the imposed parameters.

transverse compaction of the yarn and a change in the yarn cross-section. The model can be improved to properly describe the load/strain curve, for example by taking into account a change of the yarn diameter along with the increase of the contact force [27], and by introducing friction to model the nonlinear behaviour at the beginning of the test. The effect of considering a 2D knit instead of a 3D loop would also be investigated. In the course-wise direction, Fig. 4, the model is closer to the experimental data, but for a limited strain range. In the present case, the inverse method is unable to find a solution for strains higher than 0.65 in both course and wale-wise directions. The assumption of the direct model (2D loop, constant yarn diameter) are too strong for high loads that may imply a yarn transverse compaction, and significant yarn out-of-plane bending. Nevertheless it is noteworthy that this strain level seems in general high enough for the intended application (shaping of knitted preform).

Fig. 3 compares the loop shape obtained with the 2D model to a top view of the un-extended knit. A very fair agreement is observed qualitatively and provides a first validation of the model for the expected use, i.e. to feed the homogenisation model with the shape of an extended loop, as shown in Fig. 3 in the wale-wise direction, and in Fig. 4 in the course-wise direction.

## 3. Assessment of the elastic properties of the composite

This section is based on a mesoscopic homogenisation method developed by Ramakrishna et al. [16,17] to assess the elastic properties of the composite in the course and wale-wise directions. But in this study, the model takes into account the loop geometry description provided by the 2D knit extension model detailed in Section 2, instead of using the 3D geometrical model of Leaf and Glaskin [18]. On the one hand, only the in-plane elastic properties of the composite will be assessed, but on the other hand, a direct coupling with the knit extension can be performed in a simple procedure. Moreover a geometric description of the inlaid yarns is added.

The homogenisation method requires the definition of the representative volume element, RVE. The RVE depends on the fibrous architecture and on the loading direction. The RVE chosen in all cases investigated, are described further. Regardless of the RVE, the homogenisation procedure is the same. Each yarn is discretized into a large number of straight segments assumed to behave as an unidirectional lamina. The first step of the procedure is the assessment of the fibre volume fraction in the yarns, Vf_y, allowing to calculate the elastic properties of the unidirectional material.
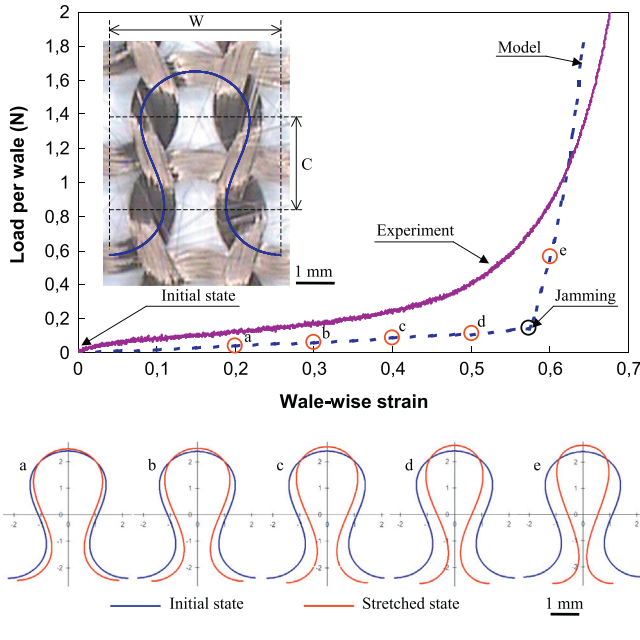
Fig. 3. Tensile behaviour in the wale-wise direction of a basalt plain-knit. Comparison of the load/strain curve and initial loop shape to experimental data and shape of the loop for several levels of deformation. (For interpretation of the references to colour in this figure legend, the reader is referred to the web version of this article.)
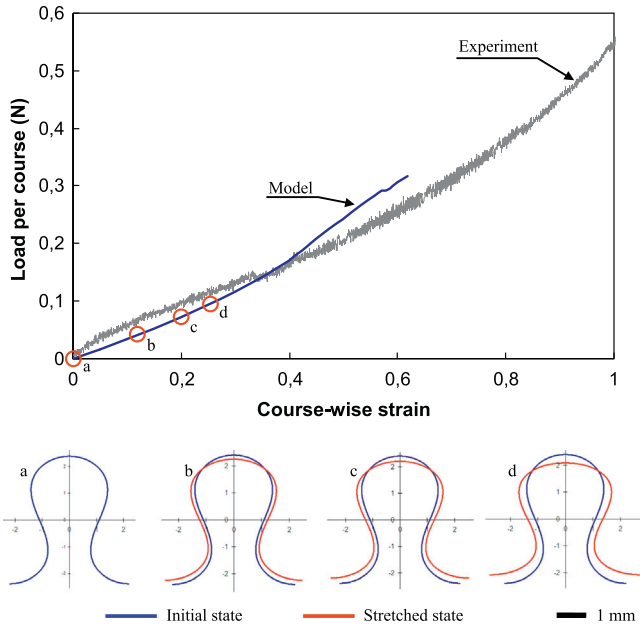
Fig. 4. Tensile behaviour in the course-wise direction of a basalt plain-knit. Comparison of the load/strain curve to experimental data and shape of the loop for several levels of deformation. (For interpretation of the references to colour in this figure legend, the reader is referred to the web version of this article.)

3.1. Micromechanical model for the impregnated yarn

The fibre volume fraction in the yarns, Vf_y, is assessed from image analysis of a cross-section of an impregnated yarn in the composite sample, Fig. 5. An average value of 65 ± 3% is measured over 9 images. Each straight segment of the discretized yarn is defined by the in-plane elastic constants of the unidirectional laminate (tensile modulus in the fibre direction E_{11} and in the transverse direction E_{22}, Poisson's ratio v_{12} and in-plane shear
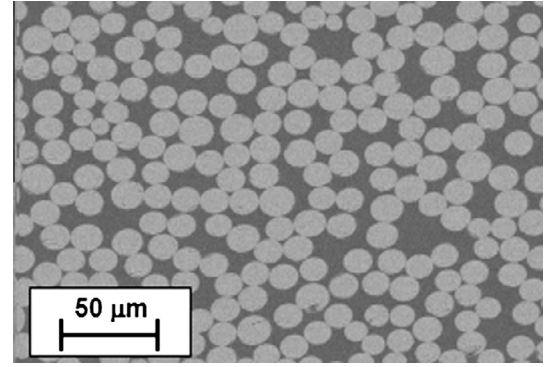
Fig. 5. Cross-section of an impregnated yarn in a composite sample (basalt–epoxy).

modulus G_{12}) and the angle between the segment k and the load direction, ψ_k. E_{11}, E_{22}, v_{12} and G_{12} are calculated from the elastic properties of the fibre and the matrix (tensile modulus, respectively E_f and E_m, Poisson's ratio, respectively v_f and v_m, and shear modulus, respectively G_f and G_m), using a homogenisation model of an unidirectional laminate (with Vf_y measured previously). Several models were tested: rule of mixtures, Chamis model [29] and Uemura model [30]. The rule of mixtures, Eqs. (12)–(15), proved to be the best suited to fit the experimental data [27] and was selected to calculate the composite properties.

$$E_{11} = Vf_y E_f + (1 - Vf_y)E_m \tag{12}$$

$$v_{12} = Vf_y v_f + (1 - Vf_y)v_m \tag{13}$$

$$E_{22} = \frac{E_m}{1 - Vf_y\left(1 - \frac{E_m}{E_f}\right)} \tag{14}$$

$$G_{12} = \frac{G_m}{1 - Vf_y\left(1 - \frac{G_m}{G_f}\right)} \tag{15}$$

In the coordinate system (X_L, Y_L) related to the load (X_L is the load direction), the elastic properties E_{Xk}, E_{Yk}, v_{XYk} and G_{XYk} of each segment k of the impregnated yarn can be obtained by Eqs. (16)–(19) as a function of the angle ψ_k.

$$\frac{1}{E_{Xk}} = \frac{\cos^4 \psi_k}{E_{11}} + \left(\frac{1}{G_{12}} - \frac{2v_{12}}{E_{11}}\right) \sin^2 \psi_k \cos^2 \psi_k + \frac{\sin^4 \psi_k}{E_{22}} \tag{16}$$

$$\frac{1}{E_{Yk}} = \frac{\sin^4 \psi_k}{E_{11}} + \left(\frac{1}{G_{12}} - \frac{2v_{12}}{E_{11}}\right) \sin^2 \psi_k \cos^2 \psi_k + \frac{\cos^4 \psi_k}{E_{22}} \tag{17}$$

$$v_{XYk} = E_{Xk}\frac{v_{12}}{E_{11}}\left(\sin^4 \psi_k + \cos^4 \psi_k\right)$$
$$- E_{Xk}\left(\frac{1}{E_{11}} + \frac{1}{E_{22}} - \frac{1}{G_{12}}\right) \sin^2 \psi_k \cos^2 \psi_k \tag{18}$$

$$\frac{1}{G_{XYk}} = 2\left(\frac{2}{E_{11}} + \frac{2}{E_{22}} + \frac{4v_{12}}{E_{11}} - \frac{1}{G_{12}}\right) \sin^2 \psi_k \cos^2 \psi_k$$
$$+ \frac{1}{G_{12}}\left(\sin^4 \psi_k + \cos^4 \psi_k\right) \tag{19}$$

Assuming a uniform strain of the RVE in the load direction, the apparent elastic properties of a yarn m, $\overline{E}_{Xm}$, $\overline{E}_{Ym}$, $\overline{v}_{XYm}$ and $\overline{G}_{XYm}$, are assessed by Eqs. (20)–(23) by averaging the properties of the n segments of length l_k, over the yarn length L_m.

$$\overline{E}_{Xm} = \frac{1}{L_m} \int_0^{L_m} E_X ds \approx \frac{1}{L_m} \sum_1^n l_k E_{Xk} \tag{20}$$

$$\overline{E}_{Ym} = \frac{1}{L_m} \int_0^{L_m} E_Y ds \approx \frac{1}{L_m} \sum_1^n l_k E_{Yk} \qquad (21)$$

$$\overline{v}_{XYm} = \frac{1}{L_m} \int_0^{L_m} v_{XY} ds \approx \frac{1}{L_m} \sum_1^n l_k v_{XYk} \qquad (22)$$

$$\overline{G}_{XYm} = \frac{1}{L_m} \int_0^{L_m} G_{XY} ds \approx \frac{1}{L_m} \sum_1^n l_k G_{XYk} \qquad (23)$$

3.2. Homogenisation at the mesoscopic scale

The representative volume element is idealized as a laminate comprised of two kinds of laminae. The first lamina corresponds to the net-matrix volume in the RVE. The elastic properties of this lamina are those of the matrix and the ratio between its thickness and the laminate thickness is $1 - Vf/Vf_y$, with Vf the fibre volume fraction in the RVE, and Vf_y the fibre volume fraction in the yarn. The other lamina corresponds to the impregnated yarns (plain knit and inlaid yarns) and their total thickness is Vf/Vf_y. Each of these lamina have the average properties of the yarn, obtained by Eqs. (20)–(23) and a thickness proportional to the length of the yarn divided by the total yarn length in the RVE. The rigidity matrix can thus be calculated for each lamina and the laminate theory allows the calculation of the composite effective properties. The next subsections details the RVE chosen in each case under study.

3.2.1. Representative volume element for plain-knit reinforced composites

The smallest periodic pattern of a plain knit includes a whole loop and the four quarters of loop in contact with it. For load directions parallel to the course or the wale-wise direction, considering the symmetries of a plain knit, this periodic pattern can be reduced to a RVE constituted on two quarters of loops in contact, and symmetric with respect to the contact point, as in Section 2 (Fig. 1).

3.2.2. Representative volume element for composites with inlaid yarns

In the present study, the inlays are tucked each four wales and float in-between. The smallest periodic pattern of a knit reinforced composite with inlaid yarns is thus a C height and $4W$ wide rectangle, Fig. 6. Each RVE of the plain knit are thus completed by one, two or three inlaid yarns. The different RVE considered for the plain-knit composites with one, two or three inlays are depicted in Fig. 6. The geometry of each inlay is described by two arcs of sinusoid tangent at point 3. From experimental observations, the length of an inlay in the RVE is 30% higher than the width of the RVE in the un-extended state. For an extended knit, the length is assumed to remain constant and the course-wise strain is assumed to be uniform over the RVE.

3.3. Results and comparison to experiment

The results of the aforementioned homogenisation model are compared to experimental data, Fig. 7, for composites reinforced with un-extended knits. The details of the composite material manufacturing, on specimen preparation and on the experimental results are available in [10]. The order of magnitude of the moduli, as well as the main trends are similar, particularly for plain knit and knit with one inlaid yarn. Nevertheless the model underestimates significantly the moduli of composites with two and three inlays, irrespective of the load direction. This can be explained by an inappropriate input data set since the model has been adjusted on the different experiments to take into account the actual thickness and fibre volume fraction. Indeed, the insertion of inlaid yarns implies a higher fibre volume fraction in the composite, and may
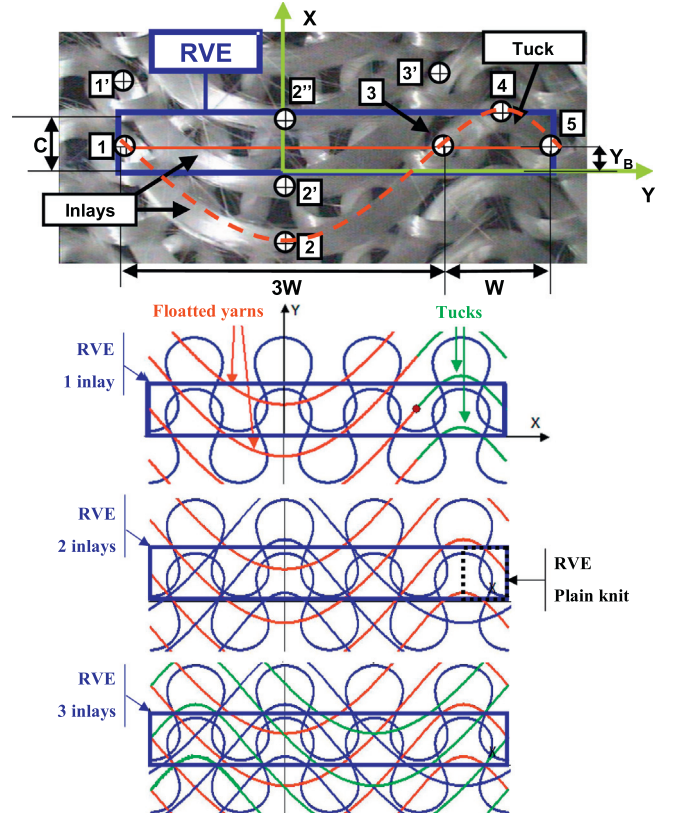
Fig. 6. RVE for the different reinforcement under study and geometric modelling of the inlaid yarns. (For interpretation of the references to colour in this figure legend, the reader is referred to the web version of this article.)

lead to a compaction of the yarns, increasing the fibre volume fraction inside the yarns, whereas this parameter was assumed to be the same irrespective of the knit. The length of the inlay may depend on the number of inlaid yarns, but it was also set to an average value.

4. Effect of stretching the preform on the elastic properties of the composite

4.1. Stretching in the wale-wise direction

Stretching the knit in the wale-wise direction, Fig. 8a and b, leads to a similar effect irrespective of the insertion of inlaid yarns. The course-wise modulus decreases slightly, whereas the wale-wise modulus increases almost linearly with the strain. An increase of 50% and even more arises for a 40% stretched knit with two or three inlays, mainly related to the inlays alignment in the loading direction.

4.2. Stretching in the course-wise direction

Stretching the knit in the course-wise direction, Fig. 8c and d, is more sensitive to the reinforcement under consideration. The wale-wise modulus decreases slightly but almost linearly with the strain, whereas the wale-wise modulus increases exponentially. An increase of 30% is obtained for a 25% stretched knit with three inlays. The effect of a course-wise stretching is mainly related to the inlays straightening, and the insertion of each inlaid yarn results in a similar effect.
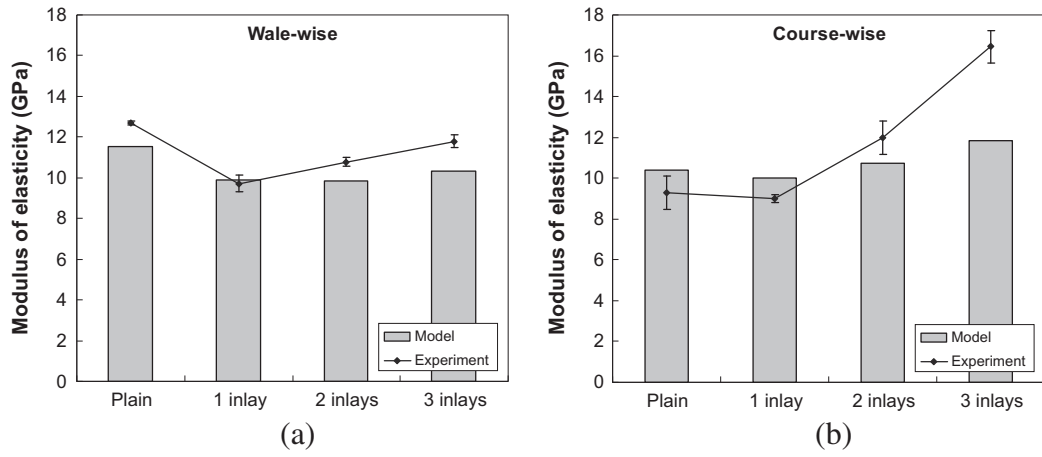
Fig. 7. Experimental and computed elasticity modulus of basalt knit reinforced composites in the wale (a) and course-wise (b) directions.
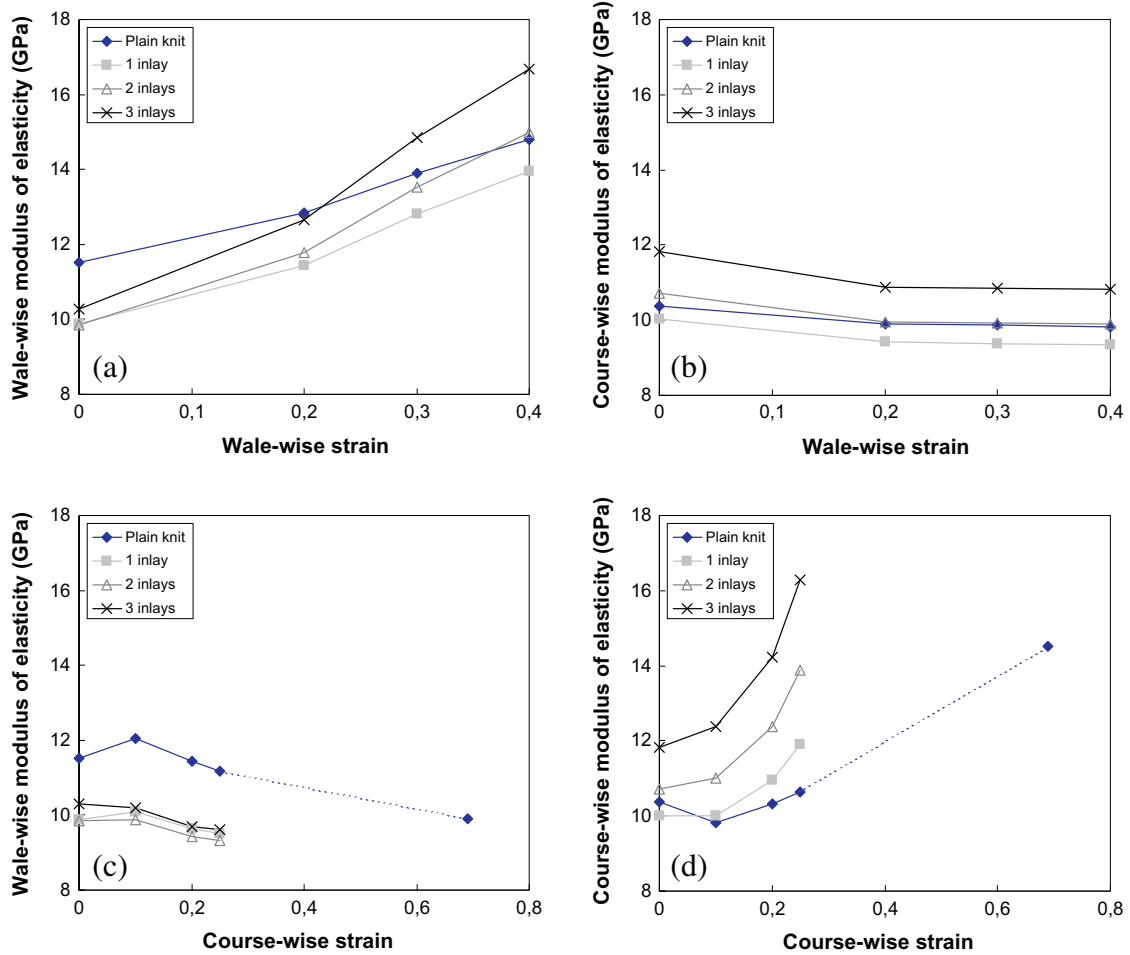

Fig. 8. Effect of a wale (a and b) and course-wise (c and d) extension of the knitted reinforcement on the wale (a and c) and course-wise (b and d) computed modulus of elasticity of the basalt knit reinforced composites. (For interpretation of the references to colour in this figure legend, the reader is referred to the web version of this article.)

4.3. Map of the wale-wise modulus versus the course-wise modulus

Fig. 9a shows a plot of the wale-wise modulus of elasticity as a function of the course-wise modulus for each configuration simulated. The main trend is similar for each reinforcement, i.e. an hyperbolic decrease of the wale-wise modulus with the course-wise modulus increase, and reciprocally. The curves are almost symmetric with respect to the bisector of the first quadrant angle (isotropic material), allowing to design a material with a given anisotropy ratio either in the wale-wise direction, or in the course-wise direction, Fig. 9b. This can be useful since it is not always possible to knit a fabric in any direction. For example, a cylindrical fabric is necessarily knitted with the axis of the cylinder parallel to the wale-wise direction.
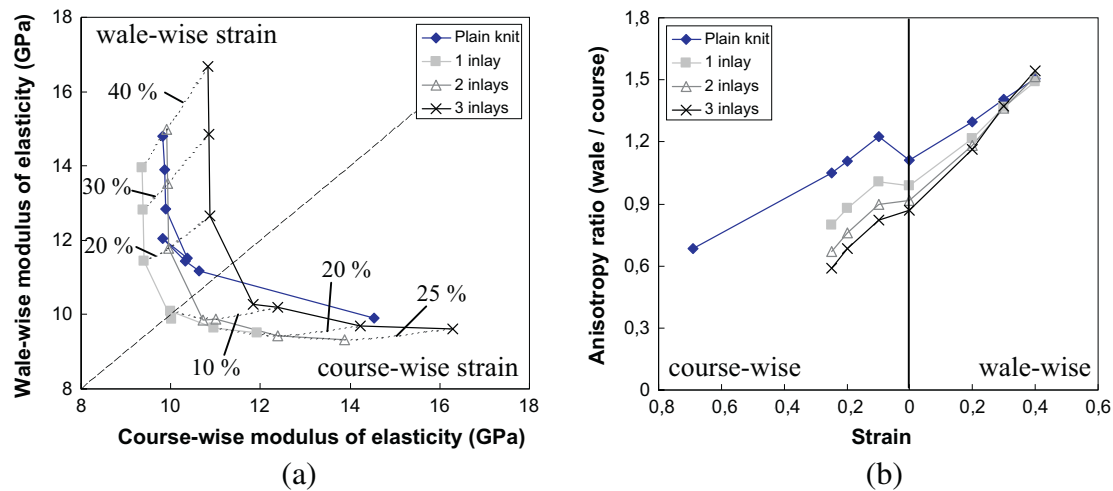
Fig. 9. Wale-wise modulus of elasticity of knit reinforced composites versus the course-wise modulus (a) and anisotropy ratio (b) for several numbers of inlaid yarns and uniaxial strain levels. (For interpretation of the references to colour in this figure legend, the reader is referred to the web version of this article.)

5. Conclusion

The model proposed in this paper couples a knit stretching model, based on the beam theory, a geometric description of the inlaid yarns, and a mesoscopic homogenisation model. The former model provides an approached load–strain curve of knitted fabrics subjected to uniaxial or biaxial elongation. An accurate description of the plane geometry of the loop is also obtained and can be used in the homogenisation model. This latter model discretizes the impregnated yarn as several straight segments of unidirectional laminates. The properties of the laminate are determined from the fibre volume fraction inside the yarn. The elastic properties of the knitted composite are assessed using the laminate theory. Good results are obtained for plain knit and knit with one inlay. For knits with two or three inlays, the main trend is observed, but the moduli of elasticity are significantly underestimated, due to inappropriate input data, identified on plain knit composites. The main contribution of this work is the coupling of both models, allowing to assess the elastic properties of composites reinforced with stretched knits: this is the major interest of this family of fabrics when manufacturing complex parts. A map of the wale-wise modulus versus the course-wise modulus has been drawn, allowing the designer to chose the knitted structure and size the preform in such a way that the strain field in the shaped preform matches the mechanical requirements in selected areas, and thus design a composite with non-uniform tailor-made elastic properties.

References

[1] Leong KH, Ramakrishna S, Huang ZM, Bibo GA. The potential of knitting for engineering composites – a review. Composites: Part A 2000;31(3):197–220.
[2] Xu W, Zhou F, Ouyang C, Ye W, Yao M, Xu B. Mechanical properties of small-diameter polyurethane vascular grafts reinforced by weft-knitted tubular fabric. J Biomed Mater Res A 2010 January;92(1):1–8.
[3] Kameo K, de Haan J, Nakai A, Hamada A. Open hole tensile behaviours of knitted fabric composites. J Reinf Plast Compos 1999;18(17):1605–13.
[4] Khondker OA, Herszberg I, Leong KH. An investigation of the structure-property relationship of knitted composites. J Compos Mater 2001;35(6): 489–508.
[5] Rozant O, Bourban PE, Manson JAE. Warp-knit laminates for stampable sandwich preforms. Compos Sci Technol 2001;61(1):145–56.
[6] Luo Y, Verpoest I. Biaxial tension and ultimate deformation of knitted fabric reinforcements. Composites: Part A 2002;33(2):197–203.
[7] Duhovic M, Bhattacharyya D. Simulating the deformation mechanisms of knitted fabric composites. Composites: Part A 2006;37(11):1897–915.
[8] Ramakrishna S, Hull D. Tensile behaviour of knitted carbon-fibre-fabric/epoxy laminates-Part I: Experimental. Compos Sci Technol 1994;50(2):237–47.
[9] Khondker OA, Fukui T, Nakai A, Hamada H. Initial fracture of the welt weft-knitted textile composites. Composites: Part A 2004;35(10):1185–94.
[10] Balea L, Dusserre G, Bernhart G. Mechanical behaviour of plain-knit reinforced injected composites: Effect of inlay yarns and fibre type. Composites: Part B 2014;56:20–9.
[11] Khondker OA, Leong KH, Herszberg I. Effects of biaxial deformation of the knitted glass preform on the in-plane mechanical properties of the composite. Composites: Part A 2001;32(10):1513–23.
[12] de Araùjo M, Fangueiro R, Hong H. Modelling and simulation of the mechanical behaviour of weft-knitted fabrics for technical applications. Part IV: 3D FEA model with a mesh of tetrahedric elements. AUTEX Res J 2004;4(2):72–80.
[13] Huang ZM, Ramakrishna S. Micromechanical modeling approaches for the stiffness and strength of knitted fabric composites: a review and comparative study. Composites: Part A 2000;31(5):479–501.
[14] Rudd CD, Owen MJ, Middleton V. Mechanical properties of weft knit glass fibre/polyester laminates. Compos Sci Technol 1990;39(3):261–77.
[15] Krenchel H. Fiber reinforcement. Copenhagen: Akademisk Forlag; 1964. p. 11–32.
[16] Ramakrishna S, Hamada H, Cheng KB. Analytical procedure for the prediction of elastic properties of plain knitted fabric-reinforced composites. Composites: Part A 1997;28(1):25–37.
[17] Ramakrishna S. Characterization and modelling of the tensile properties of plain weft-knit fabric-reinforced composites. Compos Sci Technol 1997;57(1):1–22.
[18] Leaf GAV, Glaskin A. The geometry of a plain knitted loop. J Text Inst 1955;45(9):T587–605.
[19] Hagège B, Boisse P, Billoët JL. Finite element analyses of knitted composite reinforcement at large strain. Eur J Comput Mech 2005;14(6–7):767–76.
[20] Bekisli B, Nied HF. Thermoforming of knitted composite structures: FEM simulation and experiments. Int J Mater Form 2010;3(1):615–8.
[21] de Araùjo M, Fangueiro R, Hong H. Modelling and simulation of the mechanical behaviour of weft-knitted fabrics for technical applications. Part III: 2D hexagonal fea model with non-linear truss elements. AUTEX Res J 2004;4(1):26–32.
[22] MacRory BM, McCraith JR, McNamara AB. The biaxial load-extension properties of plain, weft-knitted fabrics – a theoretical analysis. Text Res J 1975;45(10):746–60.
[23] Hepworth B, Leaf GAV. The mechanics of an idealized weft-knitted structure. J Text Inst 1976;67(7–8):241–8.
[24] Shanahan WJ, Postle R. A theoretical analysis of the tensile properties of plain-knitted fabrics. Part I: The load-extension curve for fabric extension parallel to the courses. J Text Inst 1974;65(4):200–12.
[25] Shanahan WJ, Postle R. A theoretical analysis of the tensile properties of plain-knitted fabrics. Part II: The initial load-extension behaviour for fabric extension parallel to the wales. J Text Inst 1974;65(5):254–61.
[26] Hong H, de Araujo MD, Fangueiro R, Ciobanu O. Theoretical analysis of load-extension properties of plain weft knits made from high performance yarns for composite reinforcement. Text Res J 2002;72(11):991–6.

[27] Balea L. Comportement des matériaux composites à renforts tricotés élaborés par injection de résine. PhD thesis Université de Toulouse, France; 2011 (in French).

[28] Balea L, Dusserre G, Bernhart G, Dumont N. Mechanical behaviour of technical knitted fabrics for composite applications. In: Comptes rendus des JNC-16. Toulouse; June, 2009 (in French).

[29] Chamis CC. Mechanics of composite materials: Past, present and future. J Compos Technol Res 1989;11(1):3–14.

[30] Uemura M, Ataka N, Fukuda H, Ben G. Practical FRP structural strength calculations. Japan: Japan Society of Reinforced Plastics, Ion Publishers; 1984.